


## PAPER

[View Article Online](#)  
[View Journal](#) | [View Issue](#)Cite this: *Dalton Trans.*, 2025, **54**,  
2842

# Study of the self-degradation performance of a passive direct methanol fuel cell with an Fe–N–C catalyst†

Chenjun Hou,<sup>a</sup> Weijian Yuan,<sup>a</sup>  <sup>✉</sup> Shilong Gao,<sup>b</sup> Yujun Zhang,<sup>a</sup> Yufeng Zhang<sup>a</sup> and Xuelin Zhang  <sup>✉</sup>

Fe–N–C catalysts are considered promising substitutes for Pt-based catalysts at the cathode in direct methanol fuel cells (DMFCs) owing to their great methanol tolerance. However, Fe–N–C-based DMFCs commonly suffer from a decreased performance under extremely high methanol concentrations and exhibit poor stability, while the underlying mechanism remains controversial. In this study, a self-degradation phenomenon in a passive Fe–N–C-based DMFC was investigated in detail. The DMFC with an optimized ionomer content and catalyst loading delivered an extremely high peak power density of 28.85 mW cm<sup>−2</sup> when fed with 3 M methanol solution, while the peak power density of the cell rapidly declined to 16.61 mW cm<sup>−2</sup> after standing for 10 days without any discharging operation. Several electrochemical measurements were designed and conducted to explore the mechanism for this phenomenon. The results of these measurements revealed that methanol molecules are chemically adsorbed on the surface of the Fe–N–C catalyst, and the bonding cannot be reversed using simple physical methods, leading to the isolation of active sites from oxygen. Herein, we provide a new perspective on passive Fe–N–C-based DMFCs that would be significant for the technological development of portable power devices.

Received 30th October 2024,  
Accepted 10th December 2024

DOI: 10.1039/d4dt03024a

[rsc.li/dalton](https://rsc.li/dalton)

## 1. Introduction

Globally, research on improved power supply systems has been stimulated by the ever-increasing demand for small portable electronic devices, such as smartphones, laptop computers, tablets, and global positioning systems (GPSs).<sup>1</sup> In this case, direct methanol fuel cells (DMFCs) can perfectly match the demanding requirements for energy density as well as easy and fast recharging.<sup>2</sup> Currently, platinum-based materials have long been regarded as the most effective catalysts for the methanol oxidation reaction (MOR) and oxygen reduction reaction (ORR) at the anode and cathode of DMFCs, respectively. However, the phenomenon of methanol crossover—a fraction of unreacted methanol permeating through the proton exchange membrane (PEM) from the anode to the cathode—requires Pt-based DMFCs to be usually operated in a diluted

methanol concentration of 2–5 M, thus significantly lowering energy density.

Thus, in the past decade, great efforts have been devoted to developing platinum group metal-free (PGM-free) catalysts with high activities toward the ORR. Among them, transition metal–nitrogen-containing complexes supported on carbon materials (Me–N–C, where Me = Fe, Co, Ni, *etc.*) have shown excellent performances to a level at which they can be competitive with Pt.<sup>3–6</sup> Piotr Zelenay *et al.* used polyaniline (PANI) as a nitrogen–carbon template to synthesize Fe- and Co-based ORR catalysts, where the aromatic structure of PANI was expected to stabilize the interaction between the metal and nitrogen embedded in the resulting graphitic carbon structure.<sup>7</sup> A cathode prepared with the catalysts achieved the same current densities recorded in the kinetic region at fuel cell voltages greater than 0.75 V as those obtained with a Pt cathode. Jean-Pol Dodelet *et al.* synthesized an Fe–N–C electrocatalyst *via* the pyrolysis of a mixture of a metal–organic-framework, iron acetate and phenanthroline in Ar and NH<sub>3</sub>.<sup>8</sup> The as-prepared catalyst showed an increased volumetric activity and enhanced mass transport properties, enabling the proton exchange membrane fuel cell (PEMFC) to achieve a power density of 0.75 W cm<sup>−2</sup> at 0.6 V, which is comparable with that of a commercial Pt-based fuel cell. Given that these Fe–N–C catalysts not only

<sup>a</sup>School of Astronautics, Harbin Institute of Technology, Harbin, China.

E-mail: ywj@hit.edu.cn, zhangxuelin@hit.edu.cn

<sup>b</sup>State Key Laboratory of Organic-Inorganic Composites, Beijing Advanced Innovation Center for Soft Matter Science and Engineering, Beijing University of Chemical Technology, Beijing, 100029, People's Republic of China† Electronic supplementary information (ESI) available. See DOI: <https://doi.org/10.1039/d4dt03024a>

have high ORR activity in acid but also show unique intrinsic tolerance to methanol, they can be expected to be good candidates as cathode catalysts in PEM-based DMFCs.

Although Fe–N–C catalysts have been mainly designed and tested in H<sub>2</sub>-fed PEMFCs, some works have also focused on their application in PEM-based DMFCs, as summarized in Table S1.† Among them, Shigang Sun *et al.* achieved the highest power density of 130 mW cm<sup>−2</sup> with careful design of the cathode triple-phase interface by adding hydrophobic materials to the Fe–N–C catalyst layer.<sup>9</sup> As a general observation, the power densities of the DMFCs with the Fe–N–C catalyst cathode are comparatively lower than that with a Pt cathode, as summarized in Table S2,† but a better performance could be obtained if the power density was normalized to the total Pt amount used to fabricate the membrane electrode assembly (MEA). Compared with Pt/C catalysts, Fe–N–C catalysts have different wetting properties and micropore structures, indicating that the structure of the MEA should be designed and fabricated in another way to facilitate water removal and oxygen transport, which can improve the output performance of the cell to a great extent. However, most of the published works concerning the fabrication of Fe–N–C-based DMFCs focused on cells operated in the active mode, that is, methanol solution was fed by a pump. Alternatively, only a few studies addressed passive DMFCs, which lack a liquid pump and gas blower/compressor and depend on diffusion and natural convection for fuel and oxygen supply,<sup>10</sup> making them more suitable for highly integrated electronic devices. Given that passive DMFCs show some significantly different mass transport characteristics from that in active DMFCs, their performance will be affected in some different ways by the structure of cathode catalyst layer and cell operation conditions.

Another question that should be considered is that there is still a lack of thorough investigations about how and why the performance of Fe–N–C-based DMFCs is influenced by the methanol concentration. Although Fe–N–C catalysts show great tolerance toward MOR, their ORR activity tested in oxygen-saturated 0.5 M H<sub>2</sub>SO<sub>4</sub> decreased obviously at a high methanol concentration,<sup>11</sup> and this issue should be given more attention in passive DMFCs, which are usually operated using a higher methanol concentration than active DMFCs.<sup>12</sup> Actually, the adopted methanol concentration in most of the reported DMFCs using an Fe–N–C catalyst cathode was only as high as *ca.* 10 M, at which the cells usually exhibit a worse performance than that at lower methanol concentrations.<sup>13–18</sup> Shigang Sun *et al.* investigated the effect of methanol concentration and ascribed the performance decline to the decreased hydrophobicity of the Fe–N–C catalyst at a high methanol concentration, which makes the active sites covered by the methanol solution, and thus blocks the path of oxygen transport.<sup>19</sup> It has also been reported that the limiting current density (*I*<sub>L</sub>) achieved in oxygen-saturated 0.5 M H<sub>2</sub>SO<sub>4</sub> decreases with an increase in methanol concentration,<sup>16</sup> although *I*<sub>L</sub> should increase with an increase in methanol concentration given that oxygen has a higher solubility in methanol than that in water. Shigang Sun *et al.* also studied the adsorption of methanol

molecules on Fe–N–C, and found that their adsorption in alkaline medium can greatly suppress the ORR activity by blocking the micropore transport channels for ORR-related species, while this suppression effect disappears in acidic medium.<sup>19</sup> Therefore, further studies are required to get a deep and clear understanding of the relationship between the performances of Fe–N–C-based DMFCs and methanol concentration.

Moreover, most of the Fe–N–C-based DMFCs reported in the literature usually show poor durability, that is, their output performance degraded rapidly with time when starting to discharge under a constant voltage.<sup>13,17,18,20–24</sup> Most researchers ascribed this poor durability to the problems of water removal from the cathode, which caused an increase in the diffusion of both methanol and water through the PEM.<sup>9,24</sup> Some researchers attributed the degradation in performance to the surface electrooxidation of carbon, which transforms the surface of the Fe–N–C catalyst from hydrophobic to hydrophilic, and thus causes the micropores to be flooded and oxygen transport to be blocked.<sup>21,25</sup> Actually, it should be noticed that these durability tests were carried out at a high temperature, where methanol and water preferred to be in the vapor phase, which should have little effect on blocking oxygen transport, and besides, the performance decay is very rapid at the initial discharging when there is not too much water and methanol at the cathode. In this case, to further improve the performance of the Fe–N–C cathode of passive PEM-based DMFCs, it is necessary to perform a systematic investigation to determine the process occurring at the cathode.

In this work, passive DMFCs based on the Fe–N–C catalyst at the cathode were fabricated, and key parameters including the ionomer content and the catalyst loading were researched in detail. The optimized DMFC with a high loading of 8 mg cm<sup>−2</sup> catalyst and an adequate ionomer content of 45% output a high peak power density of 28.85 mW cm<sup>−2</sup> at 60 °C, which is competitive among Fe–N–C-based DMFCs in the literature, as shown in Table S2.† Additionally, as the concentration of methanol increased from 3 M to 16 M, the peak power density of the DMFC decreased by approximately 25.9%, and rapid self-degradation in the performance of the cell was observed. To explore the underlying mechanism for this phenomenon, several electrochemical tests were designed and conducted. They revealed that the chemical adsorption of methanol occurs on the surface of the Fe–N–C catalyst, which is difficult to reverse by simple physical methods, thus leading to the isolation of the oxygen active sites. Herein, we provide new insight into the self-degradation mechanism of Fe–N–C-based passive DMFCs, which is meaningful for further research into portable power devices.

## 2. Experiment

### 2.1 Synthesis of Fe–N–C catalysts

The Fe–N–C catalyst was synthesized according to our previous study.<sup>26</sup> FeCl<sub>3</sub>, PANI and carbon black served as the iron, nitro-

gen and carbon sources, respectively. Detailed parameters are recorded in the ESI.†

## 2.2 Characterization

Scanning electron microscopy (SEM), X-ray diffraction (XRD), Raman spectroscopy, N<sub>2</sub> adsorption/desorption test and X-ray photoelectron spectroscopy (XPS) measurement were conducted for the physical and chemical characterization of the prepared catalysts. More details are recorded in the ESI.†

## 2.3 Electrochemical analysis

Electrochemical experiments were conducted based on a standard three-electrode cell, and the potentials are given relative to the reversible hydrogen electrode (RHE). In the case of the rotating disk electrode (RDE) and rotating ring disk electrode (RRDE) tests, cyclic voltammetry (CV) tests were performed first, and then staircase voltammetry (SCV) tests were conducted to record the polarization curves in O<sub>2</sub>-saturated 0.1 M HClO<sub>4</sub>. An accelerated durability test was conducted by cycling between 0.6 V and 1.0 V in O<sub>2</sub>-saturated 0.1 M HClO<sub>4</sub>. More details are recorded in the ESI.†

## 2.4 Single DMFC tests

The cathode gas diffusion electrode (GDE) was fabricated by coating the Fe–N–C catalyst ink onto the surface of carbon paper with a microporous layer. For comparison, the loading of the Pt/C-based cathode GDE was 2 Pt mg cm<sup>−2</sup> and the ionomer content was 30%. The anode GDE was composed of PtRu/C catalyst with a loading of 4 PtRu mg cm<sup>−2</sup> and the ionomer content was 30% for all the DMFCs. The cathode GDE, Nafion 117 and anode GDE were sandwiched at 15 MPa and 135 °C for 5 min to obtain an MEA with the active area of 1 cm<sup>2</sup>.

# 3. Results and discussion

## 3.1 Optimization of DMFCs with Fe–N–C catalyst

It is acknowledged that the performance of a DMFC is strongly affected by its ionomer content, which plays an important role in mass transfer. Therefore, firstly, polarization tests on DMFCs with different ionomer contents were performed. As shown in Fig. 1a, with the same catalyst loading of 4 mg cm<sup>−2</sup>, the DMFC with 45% ionomer content output the highest peak power density of 23.31 mW cm<sup>−2</sup>, while the peak power density of DMFC with 30% and 60% ionomer content only reached 18.63 mW cm<sup>−2</sup> and 15.76 mW cm<sup>−2</sup>, respectively. This is attributed to the fact that a lower ionomer content would result in lower conductivity, while an excessive ionomer content would block the nanoparticles of the catalyst and hinder the transport of oxygen. Compared with Pt/C-based DMFCs, the optimal ionomer content for Fe–N–C-based DMFCs is relatively higher, which is widely reported in the literature and summarized in Table S1.† This should be attributed to the fact that Fe–N–C catalysts commonly possess high

porosity, requiring a high ionomer content to maximize the proton connection with the electrolyte membrane.<sup>14,24</sup>

In addition to the ionomer content, the catalyst loading also plays a crucial role in catalytic activities in DMFCs, which deserves detailed investigation. Fig. 1b shows that the DMFC with a catalyst loading of 8 mg cm<sup>−2</sup> achieved the highest peak power density of 28.85 mW cm<sup>−2</sup>. When the loading increased to 12 mg cm<sup>−2</sup>, the performance of the DMFC decreased to 26.09 mW cm<sup>−2</sup> owing to the increased transfer resistance caused by the thicker CCL. To evaluate the performance, a DMFC with Pt/C CCL was manufactured for comparison. Fig. S1† shows that the peak power density of the Pt/C-based cell reached 34.94 mW cm<sup>−2</sup> when fed with 3 M methanol solution, indicating that the peak power density of the Fe–N–C-based DMFC reached over 80% of that of the Pt/C-based cell. This represents an excellent performance for an Fe–N–C-based DMFC in the literature, as recorded in Table S2.†

Given that these important parameters were optimized, the performance of the DMFC under different concentrations of methanol should be investigated. Fig. 1c demonstrates that the optimized DMFC achieved the peak power density at 3 M methanol. As the methanol concentration increased from 3 M to 16 M, the performance of the cell decreased. Notably, when the concentration of supplied methanol reached as high as 16 M, the peak power density of the cell decreased to 21.38 mW cm<sup>−2</sup>, reaching 74.1% of the peak power density at 3 M methanol. This decline in the performance of Fe–N–C-based DMFCs at high methanol concentration has also been reported in the literature;<sup>11,14,27</sup> however, the mechanism remains controversial and deserves further investigation.

It has been widely reported that the stability of Fe–N–C-based fuel cells remains an issue, primarily due to the presence of H<sub>2</sub>O<sub>2</sub> as a by-product of the incomplete four-electron transfer pathway in ORR.<sup>28–30</sup> The generated H<sub>2</sub>O<sub>2</sub> undergoes a Fenton reaction catalyzed by Fe–N–C to produce reactive oxygen species, which not only leads to the leaching of Fe atoms, but also oxidizes the carbon matrix. As a result, Fe–N–C-based fuel cells suffer from a rapid degradation in their performance within the first few hours of operation, and their output performance cannot be recovered after discharging tests. Therefore, to evaluate the stability of the optimized DMFC, a short-term discharging test was conducted. Fig. S2(a)† shows that the Fe–N–C-based cell maintained a stable performance with a constant discharging current density of 100 mA cm<sup>−2</sup> within 12 g. After this stability test, a polarization test was conducted to investigate the output performance of this cell. As shown in Fig. S2(b),† the cell retained a similar peak power density to that observed before the short-term stability test. These results confirm that the stability test did not damage the fundamental characteristics of the Fe–N–C catalyst. Following the stability test, the methanol solution in the fuel reservoir was replaced with water to restore the MEA.

Interestingly, this DMFC suffered from severe self-degradation within several days. As shown in Fig. 1d, the peak power density of the DMFC decreased from 28.85 mW cm<sup>−2</sup> to

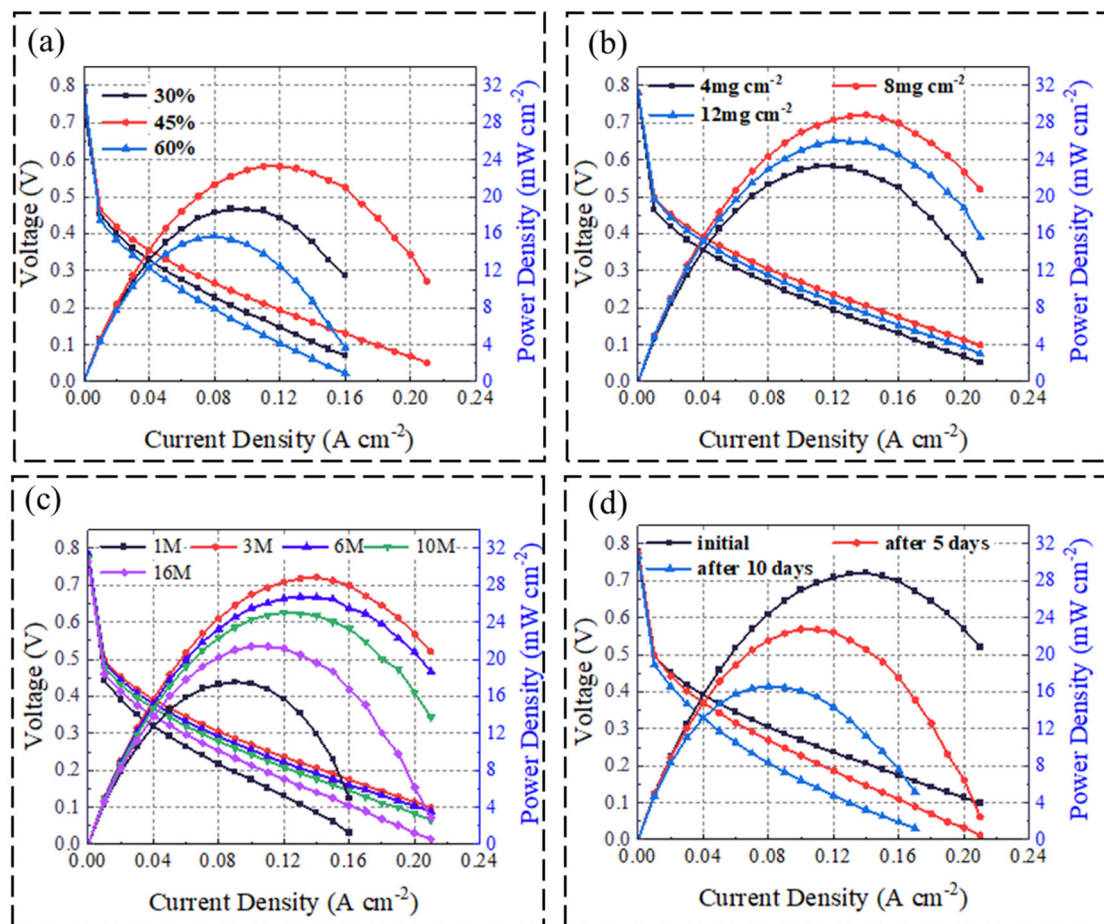


**Fig. 1** Polarization curves of an Fe-N-C-based DMFC with different ionomer contents at 3 M methanol (the loading of the Fe-N-C catalyst is  $4 \text{ mg cm}^{-2}$ ) (a). Polarization curves of the DMFC with different Fe-N-C loadings at 3 M methanol (the ionomer content is 45%) (b). Polarization curves of the DMFC with a loading of  $8 \text{ mg cm}^{-2}$  and 45% ionomer content when fed with different concentrations of methanol solution (c). Polarization curves of the DMFC at 3 M methanol within several days (d). The operation temperature is  $60^\circ\text{C}$ .

$22.72 \text{ mW cm}^{-2}$  and  $16.61 \text{ mW cm}^{-2}$  after 5 days and 10 days, respectively. In comparison, as shown in Fig. S3,<sup>†</sup> the Pt/C-based cell with the same anode and PEM showed a stable performance under the same condition. This indicates that the self-degradation mechanism is related to the Fe-N-C-based CCL.

### 3.2 Characterizations of Fe-N-C catalysts

**3.2.1 Physical characterization.** Given that the self-degradation performance of DMFCs is related to the Fe-N-C CCL, it is necessary to characterize the Fe-N-C catalyst. Fig. 2a shows the SEM image of the Fe-N-C catalyst, where the structure of the nanoparticles is related to the BP2000 carbon powder as the matrix of Fe-N-C. The XRD pattern in Fig. 2b also exhibits similar curves with two peaks at  $24.3^\circ$  and  $43.7^\circ$ , which are related to the (002) and (101) planes of carbon, respectively. The Raman spectra in Fig. 2c exhibit two prominent peaks at approximately  $1340 \text{ cm}^{-1}$  and  $1590 \text{ cm}^{-1}$ , corresponding to the D band and G band, respectively. The value of the  $I_D/I_G$  ratio was calculated to be 0.95, indicating the presence of high

carbon defects in the catalyst.  $\text{N}_2$  adsorption/desorption measurements were conducted to analyze the porous structures of the catalysts. Fig. 2d exhibits the typical IV isotherms together with the hysteric loop. Fig. S4<sup>†</sup> demonstrates the pore size distribution curve of the prepared catalyst, revealing the existence of mesoporous structures, which would expose more catalytic active sites and accelerate the mass transfer during the ORR. The Brunauer-Emmett-Teller (BET) surface area of the Fe-N-C catalyst was calculated to be  $458.27 \text{ m}^2 \text{ g}^{-1}$ . XPS measurements were conducted to analyze the chemical components in the Fe-N-C catalyst, and the nitrogen content was detected to be 1.52%. Fig. 2e reveals that the N 1s spectra could be deconvoluted into pyridinic-N, Fe-N, pyrrolic-N, graphitic-N and oxidized-N. The Fe-N-C catalyst possesses a high content of Fe-N moieties, which has been widely acknowledged as efficient ORR active sites,<sup>3,31,32</sup> indicating a good catalytic performance in ORR.

**3.2.2 Electrochemical characterization.** Besides physical characterization, electrochemical measurements were conducted to evaluate the catalytic performance of the prepared

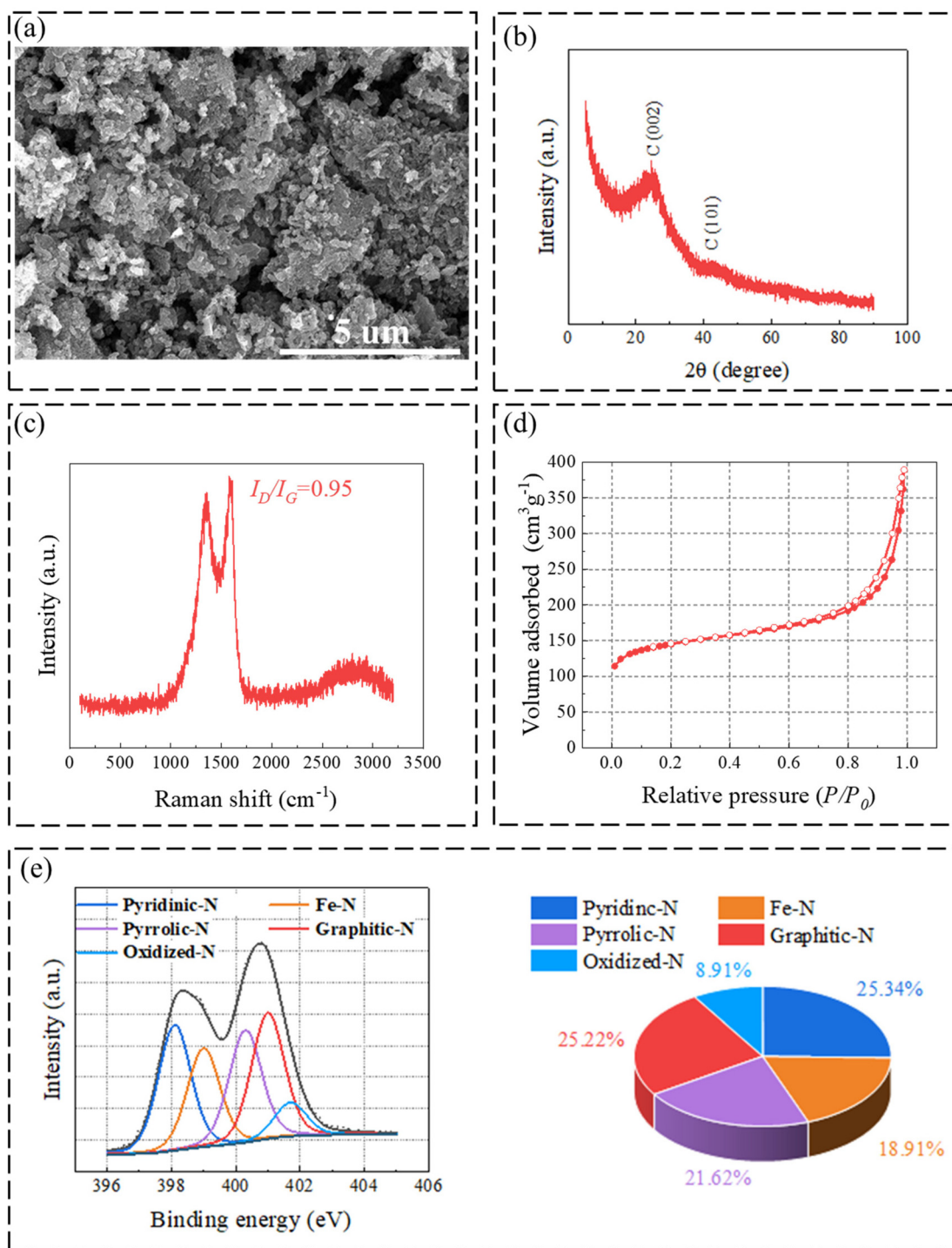


Fig. 2 SEM images (a), XRD pattern (b), Raman spectra (c),  $N_2$  adsorption/desorption isotherms (d), and XPS spectra of N 1s (e) of Fe-N-C catalysts.

catalysts. Fig. 3a shows that the Fe-N-C catalyst exhibited a high half-wave potential ( $E_{1/2} = 0.775$  V) in acidic media. Although the Fe-N-C catalyst showed an inferior catalytic performance to Pt/C, it is among the competitive Fe-N-C catalysts in the literature.<sup>33–35</sup> For further investigation of the ORR mechanism, the Tafel slopes were extrapolated from the LSV curves (Fig. S5†). As shown in Fig. 3b, the Fe-N-C catalyst

exhibited a higher Tafel slope of  $74.07 \text{ mV dec}^{-1}$  compared with Pt/C. To deeply investigate the electro-transfer process of the catalysts in ORR, SCV tests at different rotating rates were conducted. Fig. 3c and Fig. S6† show that the electron transfer number of the Fe-N-C catalyst was calculated to be 3.82 according to the Koutecky-Levich equation,<sup>36</sup> indicating high selectivity for the four-electron pathway in ORR. An RRDE

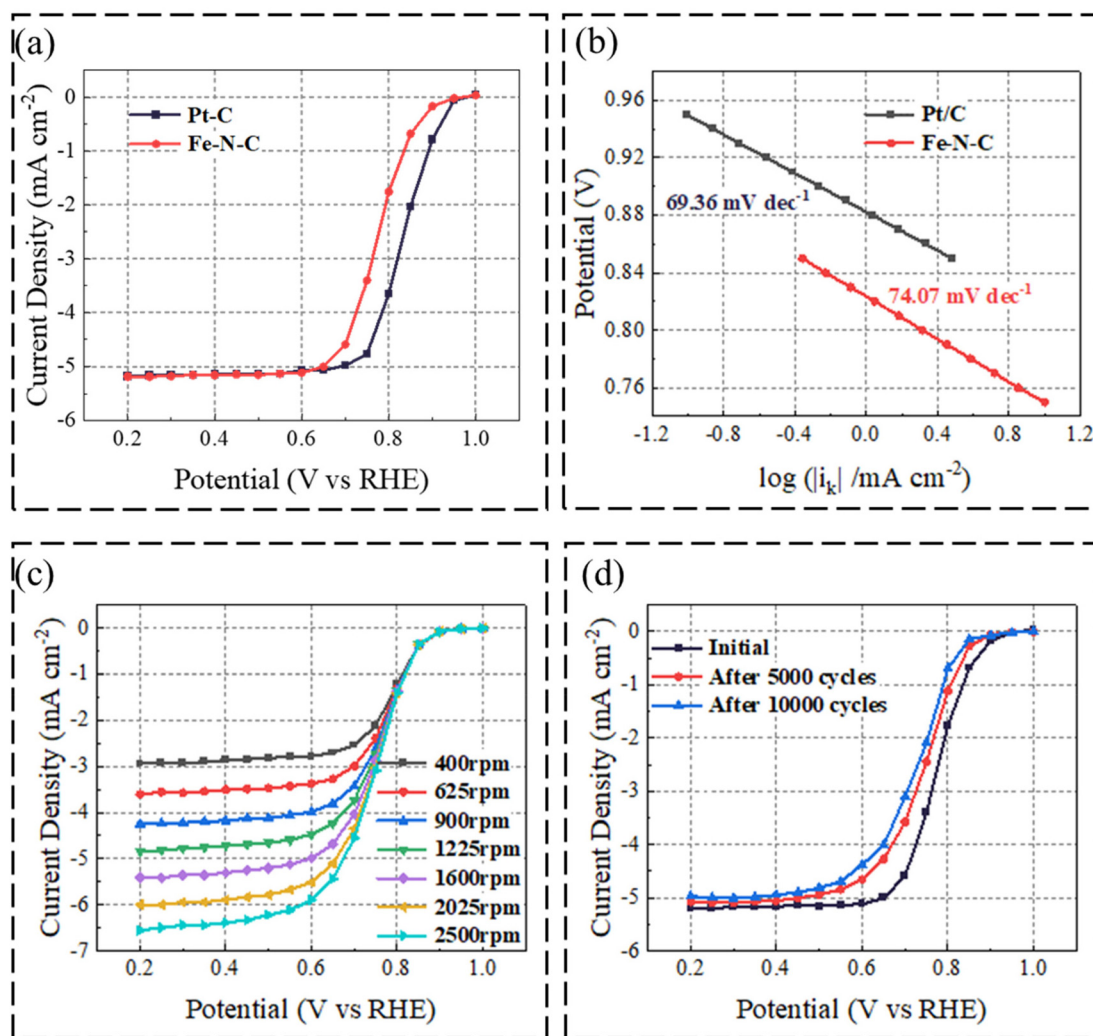


Fig. 3 SCV curves of the Fe-N-C catalyst in O<sub>2</sub>-saturated 0.1 M HClO<sub>4</sub> at 1600 rpm (a); Tafel plots of Fe-N-C catalyst in O<sub>2</sub>-saturated 0.1 M HClO<sub>4</sub> at 1600 rpm (b); SCV curves of Fe-N-C catalyst in O<sub>2</sub>-saturated 0.1 M HClO<sub>4</sub> at different rotating rates (c); SCV curves of the Fe-N-C catalyst after ADT tests (d).

test was also conducted to investigate the H<sub>2</sub>O<sub>2</sub> yield of the prepared Fe-N-C catalyst. Fig. S7† demonstrates that the H<sub>2</sub>O<sub>2</sub> yield of the prepared Fe-N-C catalyst was lower than 5% over the whole scanned potential range, revealing good selectivity for the four-electron pathway.

Additionally, an accelerated durability test was performed to evaluate the stability of the catalysts. Fig. 3d shows that a negative shift of 34 mV and 46 mV in  $E_{1/2}$  occurred for the Fe-N-C catalyst after 5000 cycles and 10 000 cycles, respectively. Besides, the chronoamperometric test of the Fe-N-C catalyst and Pt/C was performed at 0.5 V over 50 000 s. As illustrated in Fig. S8,† the Fe-N-C catalyst showed comparable stability to Pt/C. These results confirm the good catalytic stability of the prepared Fe-N-C catalyst in ORR. Considering that the ORR stability of the Fe-N-C catalyst and Pt/C is comparable, but the stability of their respective DMFCs is completely different (Fig. 1d and Fig. S3†), it can be inferred that the severe self-

degradation phenomenon observed in the DMFC is not related to the intrinsic catalytic stability of the Fe-N-C catalyst.

**3.2.3 Effect of methanol concentration on ORR performance of Fe-N-C.** As a cathode catalyst in DMFCs, the methanol tolerance of the Fe-N-C catalyst deserves further investigation. Therefore, SCV tests on the Fe-N-C based electrode were conducted in 0.1 M HClO<sub>4</sub> with varying concentrations of methanol. As shown in Fig. S9,† when the concentration of methanol was below 3 M, the Fe-N-C based electrode exhibited no apparent degradation in performance. However, when the concentration of methanol reached 5 M, an obvious shift of 63 mV in  $E_{1/2}$  was observed, as shown in Fig. 4a, accompanied by a slight decrease in the corresponding  $I_L$ , which is consistent with the related literature.<sup>11</sup> Interestingly, as the concentration of methanol increased from 5 M to 9 M, the  $E_{1/2}$  decreased slightly, while the  $I_L$  increased obviously, which seems to be a contradictory phenomenon.

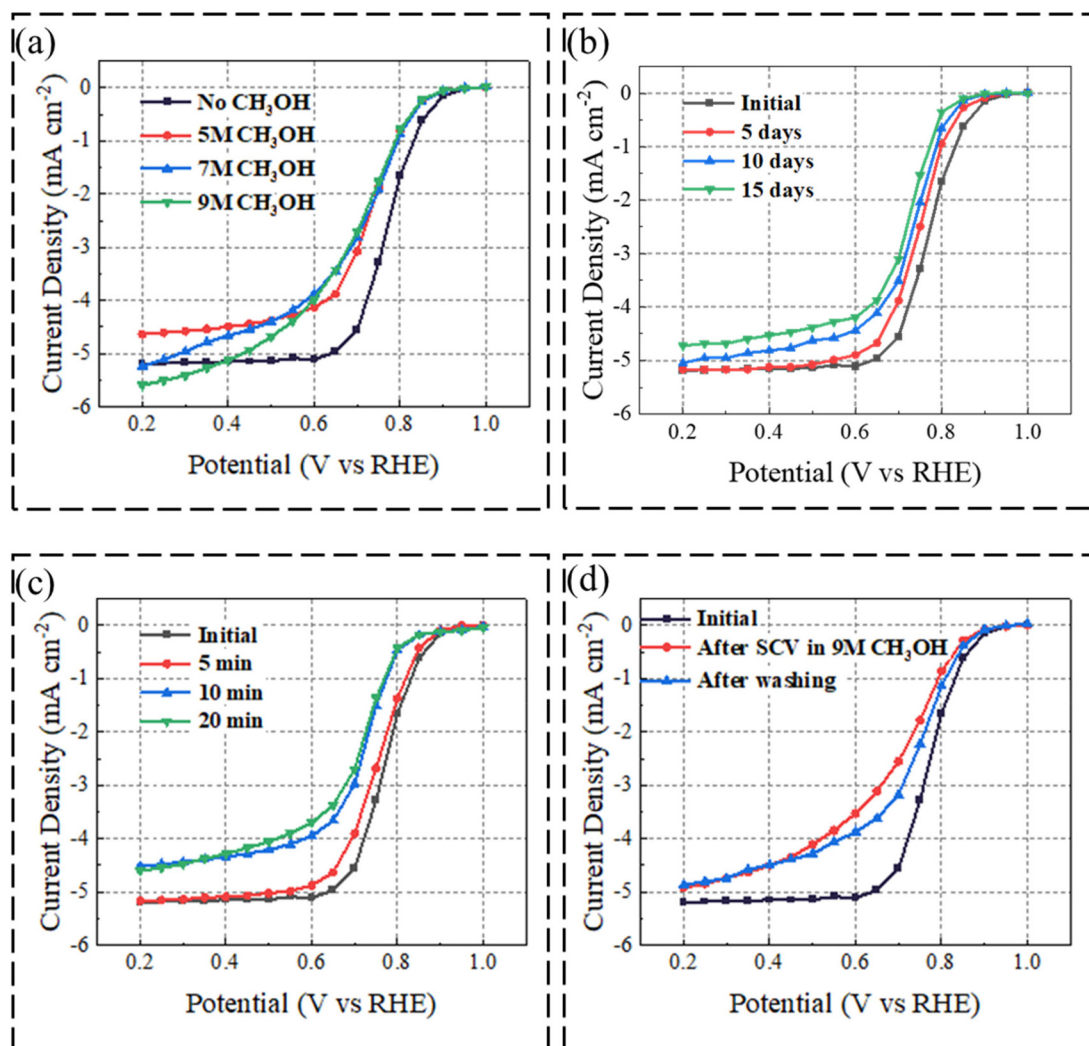


Fig. 4 SCV curves of the Fe-N-C-based electrode tested in 0.1 M HClO<sub>4</sub> with the addition of concentrated methanol (a); SCV curves of the Fe-N-C-based electrode after immersion in 0.1 M HClO<sub>4</sub> (b); SCV curves of the Fe-N-C-based electrode after immersion in 9 M methanol solution (c); SCV curves of the Fe-N-C-based electrode in 0.1 M HClO<sub>4</sub> after the SCV tests in 9 M methanol and washing treatment (d).

It has been widely acknowledged that Fe-N-C catalysts cannot catalyze the methanol oxidation reaction. Therefore, the degradation in ORR performance under concentrated methanol requires further explanation. Some researchers attributed this phenomenon to the adsorption of methanol molecules in the micropores of the Fe-N-C catalyst, which can block the oxygen transport channels to the ORR active sites, leading to a low ORR catalytic performance.<sup>19</sup> This explanation is consistent with the observed decrease in  $E_{1/2}$  and  $I_L$  tested in 5 M methanol solution. However, the increase in  $I_L$  as the methanol concentration increases is less well-explained. This phenomenon should be attributed to the higher solubility of oxygen in methanol than in water,<sup>37</sup> resulting in a higher concentration of oxygen adsorbed on the surface of the catalyst. Overall, the degradation performance of Fe-N-C-based electrodes in ORR under concentrated methanol is due to the adsorption of methanol, corresponding with a decrease in the output

peak power density of Fe-N-C-based DMFCs under a high concentration of methanol.

### 3.3 Electrochemical analysis of the self-degradation performance

It was confirmed that with the addition of concentrated methanol solution, the Fe-N-C catalyst demonstrated a significantly depressed ORR performance with a noticeable negative shift in  $E_{1/2}$ , which is attributed to the adsorption of methanol on the surface of Fe-N-C. Therefore, further electrochemical measurements should be performed to explore the mechanism for the nature of methanol adsorption. Given the fact that the Fe-N-C catalyst-based electrode was tested in HClO<sub>4</sub> together with concentrated methanol solution, it is necessary to investigate the influence of HClO<sub>4</sub> and methanol on the degradation performance of Fe-N-C, respectively.

The first validation experiment was designed and conducted to investigate the effect of  $\text{HClO}_4$  on the catalytic performance of Fe–N–C. Specifically, the Fe–N–C-based electrode was immersed in 0.1 M  $\text{HClO}_4$  for several days, after which the electrode was washed and dried. Subsequently, the dried electrode was tested in  $\text{O}_2$ -saturated 0.1 M  $\text{HClO}_4$ . As shown in Fig. 4b, after 5 days of immersion treatment, the  $E_{1/2}$  decreased from 0.775 V to 0.75 V, indicating a slight decline in ORR performance. When the immersion time was extended to 10 days and 15 days, both the  $I_L$  and  $E_{1/2}$  decreased slightly. This confirms that the  $\text{HClO}_4$  solution can slightly suppress the catalytic performance of the catalyst, which should not be the main cause for the significantly depressed catalytic performance of the Fe–N–C catalyst, as shown in Fig. 4a.

The second validation experiment was conducted to analyze the effect of methanol on the catalytic performance of the Fe–N–C catalyst. Following a similar procedure to the first validation experiment, the Fe–N–C-based electrode was immersed in 9 M methanol solution, and then washed and dried. The dried electrode was tested in  $\text{O}_2$ -saturated 0.1 M  $\text{HClO}_4$ . As shown in Fig. 4c, after 5 min of immersion, the Fe–N–C-based electrode maintained a similar ORR performance to the initial electrode without immersion treatment. However, when the immersion time increased to 10 min, the electrode exhibited a noticeable decrease in both  $I_L$  and  $E_{1/2}$ , indicating enhanced methanol adsorption. After a longer immersion treatment of 20 min, the  $I_L$  and  $E_{1/2}$  varied slightly, suggesting that the maximum methanol adsorption was reached. The shorter immersion time and the more negative  $E_{1/2}$  confirm that methanol solution plays a major role in the depressed ORR performance of the Fe–N–C catalyst compared with the  $\text{HClO}_4$  solution.

After investigating the effect of  $\text{HClO}_4$  and methanol solution on the ORR performance of the Fe–N–C catalyst, respectively, it is necessary to evaluate their corporation effect. Specifically, the Fe–N–C-based electrode was subjected to an SCV test in 0.1 M  $\text{HClO}_4$  solution with the addition of 9 M methanol for 10 min, after which the electrode was washed in deionized water and dried. As shown in Fig. 4d, after the SCV test in high-concentration methanol, the electrode exhibited a poor ORR performance with a negative  $E_{1/2}$  of 0.705 V. Following a 24 h washing treatment, the ORR performance of the electrode improved with an  $E_{1/2}$  of 0.732 V, confirming that this simple physical method is efficient in partially recovering the ORR catalytic performance. This reveals that some methanol molecules are physically adsorbed on the surface of the catalyst. However, the performance of the electrode after washing treatment remained inferior to that of the initial electrode, confirming the presence of chemically adsorbed methanol on Fe–N–C, which cannot be removed by simple physical methods.

Overall, the mechanism for the self-degradation performance of the Fe–N–C-based DMFC can be explained as follows. Due to the methanol crossover from the anode to the cathode, the ORR active sites of the Fe–N–C catalyst are occupied by adsorbed methanol molecules, leading to a decrease in the

peak power density as the supplied methanol concentration increases from 3 M to 16 M. Physically adsorbed methanol can be removed by washing treatment, which corresponds with a stable performance within the first 12 h, as shown in Fig. S2.† However, some methanol molecules are chemically adsorbed on the catalyst and cannot be recovered by simple washing treatment. Consequently, during the following several days, the Fe–N–C-based DMFC suffers from a self-degradation phenomenon, which cannot be recovered by simple physical methods.

## 4. Conclusions

Herein, a severe self-degradation phenomenon in passive direct methanol fuel cells (DMFCs) based on the Fe–N–C cathode catalyst was thoroughly investigated. The Fe–N–C-based DMFC with an adequate ionomer content of 45% and a high catalyst loading of  $8 \text{ mg cm}^{-2}$  achieved an impressive peak power density of  $28.85 \text{ mW cm}^{-2}$  when fed with 3 M methanol solution. However, its high performance rapidly declined after standing for 10 days without any operation, resulting in a significantly reduced peak power density of  $16.61 \text{ mW cm}^{-2}$ . To explore the underlying mechanism, several electrochemical measurements were designed and conducted. They confirmed that methanol molecules are chemically adsorbed on the surface of the catalyst, which cannot be reversed by simple physical methods. This leads to the isolation of the active sites from oxygen, depressing the ORR catalytic performance of the Fe–N–C catalyst seriously, and contributing to the severe self-degradation phenomenon. This study provides new insight into passive DMFCs with the Fe–N–C cathode catalyst, which is meaningful for further research on portable power devices.

## Data availability

The authors have no permission to share any data.

## Conflicts of interest

There are no conflicts to declare.

## Acknowledgements

This research was funded by the National Natural Science Foundation of China (no. 62304062 and 62274047).

## References

- 1 W. Yuan, C. Hou, X. Zhang, S. Zhong, Z. Luo, D. Mo, Y. Zhang and X. Liu, *ACS Appl. Mater. Interfaces*, 2019, **11**, 37626–37634.

- 2 T. S. Zhao, C. Xu, R. Chen and W. W. Yang, *Prog. Energy Combust. Sci.*, 2009, **35**, 275–292.
- 3 S. Zhao, Z. Ma, Z. Wan, J. Li and X. Wang, *J. Colloid Interface Sci.*, 2023, **642**, 800–809.
- 4 Y.-T. Zhang, S.-Y. Li, N.-N. Zhang, G. Lin, R.-Q. Wang, M.-N. Yang and K.-K. Li, *New Carbon Mater.*, 2023, **38**, 200–209.
- 5 Y. Zeng, C. Li, B. Li, J. Liang, M. J. Zachman, D. A. Cullen, R. P. Hermann, E. E. Alp, B. Lavina, S. Karakalos, M. Lucero, B. Zhang, M. Wang, Z. Feng, G. Wang, J. Xie, D. J. Myers, J.-P. Dodelet and G. Wu, *Nat. Catal.*, 2023, **6**, 1215–1227.
- 6 F. X. Ma, Z. Q. Liu, G. Zhang, H. S. Fan, Y. Du, L. Zhen and C. Y. Xu, *Small*, 2023, **19**, 2207991.
- 7 G. Wu, K. L. More, C. M. Johnston and P. Zelenay, *Science*, 2011, **332**, 443–447.
- 8 R. Chenitz, U. I. Kramm, M. Lefèvre, V. Glibin, G. Zhang, S. Sun and J.-P. Dodelet, *Energy Environ. Sci.*, 2018, **11**, 365–382.
- 9 Y.-C. Wang, L. Huang, P. Zhang, Y.-T. Qiu, T. Sheng, Z.-Y. Zhou, G. Wang, J.-G. Liu, M. Rauf, Z.-Q. Gu, W.-T. Wu and S.-G. Sun, *ACS Energy Lett.*, 2017, **2**, 645–650.
- 10 T. S. Zhao, R. Chen, W. W. Yang and C. Xu, *J. Power Sources*, 2009, **191**, 185–202.
- 11 Q. Li, T. Wang, D. Havas, H. Zhang, P. Xu, J. Han, J. Cho and G. Wu, *Adv. Sci.*, 2016, **3**, 1600140.
- 12 M. A. Abdelkareem, A. Allagui, E. T. Sayed, M. El Haj Assad, Z. Said and K. Elsaid, *Renewable Energy*, 2019, **131**, 563–584.
- 13 D. Sebastián, A. Serov, I. Matanovic, K. Artyushkova, P. Atanassov, A. S. Aricò and V. Baglio, *Nano Energy*, 2017, **34**, 195–204.
- 14 J. C. Park and C. H. Choi, *J. Power Sources*, 2017, **358**, 76–84.
- 15 E. Negro, A. H. A. M. Videla, V. Baglio, A. S. Aricò, S. Specchia and G. J. M. Koper, *Appl. Catal., B*, 2015, **166–167**, 75–83.
- 16 Q. Li, T. Wang, D. Havas, H. Zhang, P. Xu, J. Han, J. Cho and G. Wu, *Adv. Sci.*, 2016, **3**, 1600140.
- 17 D. Sebastián, V. Baglio, A. S. Aricò, A. Serov and P. Atanassov, *Appl. Catal., B*, 2016, **182**, 297–305.
- 18 D. Sebastián, A. Serov, K. Artyushkova, P. Atanassov, A. S. Aricò and V. Baglio, *J. Power Sources*, 2016, **319**, 235–246.
- 19 Y.-C. Wang, Y.-J. Lai, L.-Y. Wan, H. Yang, J. Dong, L. Huang, C. Chen, M. Rauf, Z.-Y. Zhou and S.-G. Sun, *ACS Energy Lett.*, 2018, **3**, 1396–1401.
- 20 D. Sebastian, A. Serov, K. Artyushkova, J. Gordon, P. Atanassov, A. S. Arico and V. Baglio, *ChemSusChem*, 2016, **9**, 1986–1995.
- 21 L. Osmieri, R. Escudero-Cid, M. Armandi, P. Ocón, A. H. A. Monteverde Videla and S. Specchia, *Electrochim. Acta*, 2018, **266**, 220–232.
- 22 Y. Hu, J. Zhu, Q. Lv, C. Liu, Q. Li and W. Xing, *Electrochim. Acta*, 2015, **155**, 335–340.
- 23 L. Osmieri, R. Escudero-Cid, M. Armandi, A. H. A. M. Videla, J. L. G. Fierro, P. Ocon and S. Specchia, *Appl. Catal., B*, 2017, **205**, 637–653.
- 24 L. Osmieri, R. Escudero-Cid, A. H. A. Monteverde Videla, P. Ocón and S. Specchia, *Appl. Catal., B*, 2017, **201**, 253–265.
- 25 G. Zhang, R. Chenitz, M. Lefèvre, S. Sun and J.-P. Dodelet, *Nano Energy*, 2016, **29**, 111–125.
- 26 C. Hou, W. Yuan, Y. Zhang, Y. Li, H. Wang, N. Xu, B. Zhang, Y. Zhang and X. Zhang, *Fuel*, 2025, **379**, 133111.
- 27 R. Mei, J. Xi, L. Ma, L. An, F. Wang, H. Sun, Z. Luo and Q. Wu, *J. Electrochem. Soc.*, 2017, **164**, F1556–F1565.
- 28 Y. Shao, J. P. Dodelet, G. Wu and P. Zelenay, *Adv. Mater.*, 2019, **31**, e1807615.
- 29 D. Banham, S. Ye, K. Pei, J.-I. Ozaki, T. Kishimoto and Y. Imashiro, *J. Power Sources*, 2015, **285**, 334–348.
- 30 M. A. Ud Din, M. Idrees, S. Jamil, S. Irfan, G. Nazir, M. A. Mudassir, M. S. Saleem, S. Batool, N. Cheng and R. Saidur, *J. Energy Chem.*, 2023, **77**, 499–513.
- 31 L. Zhang, Q. Meng, R. Zheng, L. Wang, W. Xing, W. Cai and M. Xiao, *Nano Res.*, 2023, **16**, 4468–4487.
- 32 K. Wang, H. Yang, Q. Wang, J. Yu, Y. He, Y. Wang, S. Song and Y. Wang, *Adv. Energy Mater.*, 2023, **13**, 2204371.
- 33 H. Shen, E. Gracia-Espino, J. Ma, K. Zang, J. Luo, L. Wang, S. Gao, X. Mamat, G. Hu, T. Wagberg and S. Guo, *Angew. Chem., Int. Ed.*, 2017, **56**, 13800–13804.
- 34 Z. Zhang, J. Sun, F. Wang and L. Dai, *Angew. Chem., Int. Ed.*, 2018, **57**, 9038–9043.
- 35 L. Yang, D. Cheng, H. Xu, X. Zeng, X. Wan, J. Shui, Z. Xiang and D. Cao, *Proc. Natl. Acad. Sci. U. S. A.*, 2018, **115**, 6626–6631.
- 36 C. Hou, X. Zhang, W. Yuan, Y. Zhang, H. Deng and X. Liu, *Int. J. Energy Res.*, 2021, **45**, 19574–19585.
- 37 J. Tokunaga, *J. Chem. Eng. Data*, 1975, **20**, 41–46.